Journal of Hydraulic Structures
J. Hydraul. Struct., 2021; 7(4):26-44
DOI: 10.22055/jhs.2022.40210.1202

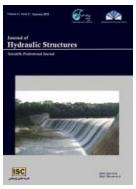

OPEN ACCESS

Theoretical Analysis and Numerical Simulation of Mechanical Energy Loss of Turbulent Flows in Open-Channel Expansions

Mahsa Mahmoudi [1]
Mohammad Ali Banihashemi[2]

Abstract

It is a popular fact that mechanical processes are usually accompanied by the dissipation phenomenon. Therefore, it is not possible to retain the initial energy over a temporal period or a local distance without spending additional energy. Because these motions are accompanied by conversion into heat. In other words, due to some factors such as friction, cross-section changes, etc., there are some energy losses that the process is irreversible, and some of the system's energy is mainly dissipated as heat. In the most cases of the open-channel transitions, the energy losses of turbulent flows are so complex that it is not easy to define specific relationships for them, and the energy losses are usually determined empirically or experimentally. Examining how the mechanical energy loss of three-dimensional turbulent flows can be estimated without measurements is one of the important subjects of this paper. In this study, in order to better understand the mechanism of the energy losses, during a journey from hydrodynamics to hydraulics, the process of the energy loss of turbulent flows and its relationship with the turbulence parameters are examined through theoretical analysis and 3-D numerical simulations. The relationship between the mechanical energy loss and the roughness coefficient is further obtained and investigated. The results are presented in the form of the application of the new analytical relationships in open-channel expansions and determining the contribution of the effective parameters of turbulent flows to the energy loss.

Keywords: Energy Loss, Turbulent Flows, Theoretical Analysis, Open-Channel Expansions, Numerical Simulations.

Received: 03 February 2022; Accepted: 06 March 2022

1. Introduction

In Hydraulics and Fluid Mechanics, two kinds of energy losses are distinguished: friction (viscous) loss and form (local) loss. On the one hand, there are losses due to wall boundaries, having close connection with the viscosity and the condition of the walls. On the other hand, losses also arise due to changes in the cross-section of the flow. Whenever the flow accelerates

[1] School of Civil Engineering, College of Engineering, University of Tehran, Tehran, Iran. E-mail: mahsa.mahmoudi@ut.ac.ir **(Corresponding author)**
[2] School of Civil Engineering, College of Engineering, University of Tehran, Tehran, Iran.

or decelerates, separation occurs and mechanical energy from the flow is withdrawn by large scale eddies. The friction (viscous) loss is produced by shear stresses along the walls, while the form (local) loss arises from internal stresses [1].

Form losses occur wherever the streamlines are directed away from the axial direction of flow owing to a change in the geometry [1]. In the case of local turbulence, these perturbations, in the form of local eddies, usually cause energy losses. The theoretical analysis of these phenomena and the study of the appeared eddies are difficult. Because these currents are not one or two-dimensional and there are no simple theories for their analysis. Hydraulic engineers usually express the energy loss as an empirical coefficient of the velocity head [2– 4], and measuring the energy loss and its expression in the form of a formula are not easy. Numerous studies have been conducted in the investigation of the turbulent flows in rivers, open-channels, and flumes with the irregular geometries [5]. Many researchers such as Nezu and Nakagawa [6], Amara et al. [7] and Haque [8] studied about the turbulent flows in the irregular channels with expansions in the vertical and transverse directions and some details of the turbulent flow were analyzed; however, their goal was not to calculate the energy losses. Previously, other researchers such as Henderson [9], Chow [4], Fouladi Nashta and Garde [10], etc. provided analytical and experimental relationships for calculating energy loss in transitions without considering the details of the turbulent flows.

Another group of studies have focused on designing the open-channel transitions with the minimum energy loss and maximum efficiency. For example, Basak and Alauddin [11] presented the results of the experimental investigations on flow through expansive transitions in rectangular rigid-bed channels. The velocity distributions of flow through the transitions were analyzed and the efficiencies of the transitions were evaluated which indicated that the model proposed by Basak and Alauddin [11] had the maximum efficiency. Najafi-Nejad-Nasser and Li [12], by using an experimental model and theoretical study, obtained the energy loss coefficients in open-channel expansions and recommended that the use of a triangular hump can effectively reduce the loss coefficients. These types of studies were often performed experimentally with the aim of controlling and reducing the energy loss based on the common 1-D energy equation. Hence, they did not include the details of the energy loss and the effect of the turbulence parameters on it. The following are some examples of the studies related to energy loss formulation.

An analytical method was proposed by Artichowicz and Sawicki [13] for estimation of the energy loss based on the energy dissipation relationship in the basic source of fluid mechanics, in which the power of the energy dissipation in steady turbulent flow can be determined based on the mean flow velocity and turbulent viscosity coefficient. The proposed method is mainly related to the pipe flow with simple geometry and its application was investigated in a circular pipe that led to inappropriate agreement between the results in turbulent flows.

Liu et al. [14] derived an energy equation using the Navier-Stokes equations for steady incompressible flows, in which the turbulence parameters in the energy loss relationship were considered. However, the application of the relationship was investigated for a uniform flow in a prismatic rectangular open-channel without existing any factors of causing additional energy loss. Therefore, many terms containing the turbulence effects were assumed to be zero.

Liu and Xue [15] numerically and analytically investigated the mechanical energy loss obtained from the mean flow energy equation and the wall resistance in steady open-channel flows. The mean flow energy equation proposed by Liu and Xue [15] was obtained by the dot

product of the mean velocity vector with *RANS*[3] equations which is not equivalent to the total flow energy equation used in the present study. In other words, in the energy equation applied by Liu and Xue [15], the variations of the turbulent kinetic energy, the work done by the viscous diffusion of the turbulent energy, and the turbulent diffusion were not taken into account. However, these terms are considered and investigated in the total mechanical energy equation proposed in this study.

Generally, in most cases of the transitions, the losses are so complex that it is not easy to define specific relationships for them, and the (local) energy loss is usually determined empirically or experimentally. The most important goal of the present study is to achieve a deeper understanding of the details of the energy losses and the mechanical energy balance in 3-D open-channel turbulent flows. These details have not been studied and analyzed in the previous energy equations applied in the open-channels.

In this study, in order to better understand the mechanism of the energy loss, during a journey from hydrodynamics to hydraulics, the process of the energy loss of open-channel turbulent flows and its relationship with the turbulence parameters are examined through theoretical analysis and three-dimensional numerical simulations. The relationship between the mechanical energy loss and the roughness coefficient is further analyzed. The results are investigated using the application of the new analytical relationships in open-channel expansions and determining the contribution of the turbulence parameters to the total energy loss, without measurements.

2. Material and methods

2.1. Mathematical Formulation

In the present study, a control volume V as shown in Fig. 1 is considered with the outer boundaries composed of S_1 and S_2 at the upstream and downstream, the channel wall S_3 and the free surface S_4 (θ is the angle between x_1-direction and the horizontal plane in Fig. 1).

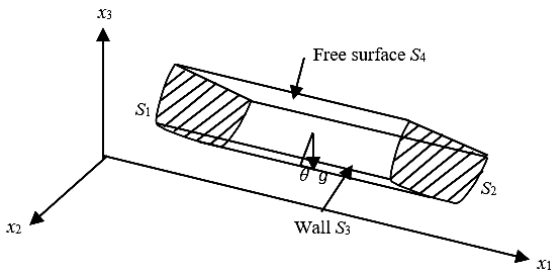

Figure 1. Schematic of the open-channel flow

As a starting point for the analysis of the total mechanical energy balance in incompressible turbulent flows, the basic method proposed by Hinze [16] and Liu et al. [14] is used. A brief outline of this method is given as follows.

By writing the Navier-Stokes equation as:

$$\frac{\partial}{\partial x_j}\rho u_i u_j = -\frac{\partial p}{\partial x_i} + \frac{\partial \tau_{ij}}{\partial x_j} + \rho f_i \qquad (1)$$

and considering Eqs. (2a) and (2b), the total energy equation (Eq. 3) is obtained from the dot product of the velocity vector with the Navier-Stokes equation:

[3] Reynolds averaged Navier-Stokes

$$\rho f_i = \frac{\partial}{\partial x_i}[\rho(-g x_3 \cos\theta + g x_1 \sin\theta)] \tag{2a}$$

$$\rho u_i \frac{\partial u_i u_j}{\partial x_j} = \frac{\partial}{\partial x_i}\left(\frac{1}{2}\rho u_j u_j u_i\right), u_i \frac{\partial \tau_{ij}}{\partial x_j} = \frac{\partial \tau_{ij} u_j}{\partial x_i} - \tau_{ij} s_{ij} \tag{2b}$$

$$\frac{\partial(\frac{\rho u_j u_j u_i}{2})}{\partial x_i} = -\frac{\partial(u_i p)}{\partial x_i} + \frac{\partial(\tau_{ij} u_j)}{\partial x_i} - \tau_{ij} s_{ij} + \frac{\partial}{\partial x_i}[\rho u_i g(x_1 \sin\theta - x_3 \cos\theta)] \tag{3}$$

where ρ, u_i, p, $\tau_{ij} = 2\mu s_{ij}$, f_i and s_{ij} are the liquid density, the instantaneous velocity and pressure, the viscous shear stress tensor, the unit mass force and the strain rate tensor, respectively. By applying Reynolds decomposition ($u_i = \overline{u_i} + u_i^{'}, p = \bar{p} + p^{'}, \tau_{ij} = \overline{\tau_{ij}} + \tau_{ij}^{'}$) to Eq. (3), then time averaging, Eq. (4) is obtained:

$$\begin{aligned}&\frac{\partial}{\partial x_i}\left[\rho\overline{u_i}\left(g x_3 \cos\theta - g x_1 \sin\theta + \frac{p_s}{\rho} + \frac{1}{2}\overline{u_j u_j} + \frac{1}{2}\overline{u_j^{'} u_j^{'}}\right)\right] = \frac{\partial(\overline{\tau_{ij} u_j})}{\partial x_i} - \overline{\tau_{ij} s_{ij}} + \\ &\frac{\partial(\overline{\tau_{ij}^{'} u_j^{'}})}{\partial x_i} - \overline{\tau_{ij}^{'} s_{ij}^{'}} - \frac{\partial}{\partial x_i}\left[\overline{p^{'} u_i^{'}} + \rho\left(\frac{1}{2}\overline{u_i^{'} u_j^{'} u_j^{'}} + \overline{u_j}\,\overline{u_i^{'} u_j^{'}}\right) + (\bar{p} - p_s)\overline{u_i}\right]\end{aligned} \tag{4}$$

In Eq. (4), p_s represents the hydrostatic pressure. In 3-D turbulent flows due to the existence of the secondary currents and the anisotropic turbulent diffusion, the assumption of the hydrostatic pressure distribution is not always satisfied [14]. Therefore, the mean pressure $\bar{p}$ is not always equal to the hydrostatic pressure p_s, and in the present energy equation, the difference of the mentioned pressures is also considered.

Integrating Eq. (4) over the total control volume and using the Gaussian theorem to transform the volume integrals into the surface integrals yields:

$$\begin{aligned}&\oiint_S \left(g x_3 \cos\theta - g x_1 \sin\theta + \frac{p_s}{\rho} + \frac{1}{2}\overline{u_j u_j} + \frac{1}{2}\overline{u_j^{'} u_j^{'}}\right)(\rho\overline{u_i} n_i) dA \\ &\qquad = -\iiint_V (\overline{\tau_{ij} s_{ij}} + \overline{\tau_{ij}^{'} s_{ij}^{'}}) dV \\ &\qquad + \oiint_S \left[-(\bar{p} - p_s)\overline{u_i} + \left(\overline{\tau_{ij} u_j} + \overline{\tau_{ij}^{'} u_j^{'}}\right) - \overline{p^{'} u_i^{'}}\right. \\ &\qquad \left. - \rho\left(\frac{1}{2}\overline{u_i^{'} u_j^{'} u_j^{'}} + \overline{u_j}\,\overline{u_i^{'} u_j^{'}}\right)\right] n_i dA\end{aligned} \tag{5}$$

Assuming $g x_3 \cos\theta - g x_1 \sin\theta + \frac{p_s}{\rho} = g z + \frac{p_s}{\rho}$ to be constant on each cross-section, using the continuity equation as $Q = \iint_{S_2} \overline{u_i} n_i dA = -\iint_{S_1} \overline{u_i} n_i dA$ and defining the mean kinetic energy correction coefficients α_1 and α_2, and the turbulent kinetic energy correction coefficients β_1 and β_2 from Eqs. (6a) and (6b), the simplified form of energy equation (Eq. 7) is obtained (where the numbers inside the parentheses represent the cross-sections S_1 and S_2):

$$\alpha_1 U_1^3 A_1 = \alpha_1 Q U_1^2 = -\iint_{S_1} \overline{u_i u_j u_j} n_i \, dA, \alpha_2 U_2^3 A_2 = \alpha_2 Q U_2^2 = \iint_{S_2} \overline{u_i u_j u_j} \, n_i dA \tag{6a}$$

$$\beta_1 U_1 k_1 A_1 = -\frac{1}{2}\iint_{A_1} \overline{u_j^{'} u_j^{'}}\,\overline{u_i} n_i dA, \beta_2 U_2 k_2 A_2 = \frac{1}{2}\iint_{A_2} \overline{u_j^{'} u_j^{'}}\,\overline{u_i} n_i dA \tag{6b}$$

$$\underbrace{z_1+\frac{p_{s1}}{\rho g}}_{1(1)}+\underbrace{\alpha_1\frac{U_1^2}{2g}}_{2(1)}+\underbrace{\beta_1\frac{k_1}{g}}_{3(1)}+\underbrace{h_{sfd1}}_{4(1),6(1),8(1),9(1),10(1)}=\underbrace{z_2+\frac{p_{s2}}{\rho g}}_{1(2)}+\underbrace{\alpha_2\frac{U_2^2}{2g}}_{2(2)}+\underbrace{\beta_2\frac{k_2}{g}}_{3(2)}+\underbrace{h_{sfd2}}_{4(2),6(2),8(2),9(2),10(2)}+\underbrace{h_w}_{5,7} \tag{7}$$

Eq. (7) is the integral form of the total mechanical energy equation for open-channel turbulent flows in which the effects of variations of the turbulent kinetic energy (term 3) and other turbulence parameters such as the viscous diffusion of the turbulent energy (term 6), the turbulent diffusion (term 8), etc. in h_{sfd}, that have not been considered in the previous energy equations, are taken into account. h_w and h_{sfd} are defined based on Eq. (5) as follows:

$$h_w=\frac{1}{\rho g Q}\iiint_V(\underbrace{\overline{\tau_{ij}s_{ij}}}_{5}+\underbrace{\overline{\tau_{ij}'s_{ij}'}}_{7})dV \tag{8a}$$

$$h_{sfd}=-\frac{1}{\rho g Q}\{\iint_S[\underbrace{-(\overline{p}-p_s)\overline{u_i}}_{10}+\underbrace{\overline{\tau_{ij}}\,\overline{u_j}}_{4}\underbrace{-\rho\overline{u_j}\,\overline{u_i'u_j'}}_{9}]n_i dA+\iint_S[\underbrace{\overline{\tau_{ij}'u_j'}}_{6}\underbrace{-\overline{p'u_i'}-\frac{1}{2}\rho\overline{u_i'u_j'u_j'}}_{8}]n_i dA\} \tag{8b}$$

All terms in Eqs. (7) and (8) are described below. From a physical perspective, $h_w$denotes the flow mechanical energy loss that can be calculated directly from Eq. (8a) or based on the difference of the other parameters in Eq. (7), while h_{sfd}represents the energy term induced by a variation of the surface forces (including the dynamic pressure, the shear stress, the Reynolds stress), the viscous diffusion of the turbulent energy and the turbulent diffusion on the inlet and outlet cross-sections.

It should be noted that it is not easy to calculate each term of the total mechanical energy equation improved in this study in the primary form (Eq. 7) due to the presence of unknown correlations such as ones described in Eqs. (8a, 8b). To overcome this, the use of equalizations is proposed (Eqs. 9-13), which provides the ability to replace the correlation of the turbulence parameters with a combination of the mean flow variables and known turbulence parameters obtained from the simulation results such as k, ε, etc.

About terms 5 and 7 in Eq. (8a) involving the physical concepts of the rate of the viscous dissipation of the mean flow energy and the dissipation rate of turbulence kinetic energy which are converted into heat, with the definition of the turbulent energy dissipation rate ($\varepsilon=2\nu\overline{s_{ij}'s_{ij}'}$), Eq. (8a) can be expressed as follows:

$$\frac{1}{\rho g A_1 U_1}\iiint_V(\overline{\tau_{ij}s_{ij}}+\overline{\tau_{ij}'s_{ij}'})dV\equiv\frac{1}{2gQ}\iiint_V\left[\nu\left(\frac{\partial\overline{u_i}}{\partial x_j}+\frac{\partial\overline{u_j}}{\partial x_i}\right)\left(\frac{\partial\overline{u_i}}{\partial x_j}+\frac{\partial\overline{u_j}}{\partial x_i}\right)+2\varepsilon\right]dV \tag{9}$$

in which, ε is obtained from Eq. (17) (more precisely, term 7 is dissipation rate at which fluctuating viscous stresses ($\nu s'_{ij}$) perform deformation work against the fluctuating strain rate (s'_{ij})).

Term 4 in Eq. (8b), which indicates the work done by viscous shear stresses, is in the form of the mean parameters and its integral can be rewritten as follows:

$$-\frac{1}{\rho g A_1 U_1}\left[\iint_{S_1}\overline{\tau_{ij}u_j}n_i dA+\iint_{S_2}\overline{\tau_{ij}u_j}n_i dA\right]$$
$$=-\frac{1}{\rho g A_1 U_1}\left[\iint_{S_1}2\mu\overline{s_{ij}u_j}n_i dA+\iint_{S_2}2\mu\overline{s_{ij}u_j}n_i dA\right]= \quad (10)$$
$$-\frac{1}{gQ}\left[\iint_{S_1}\overline{u_j}\nu(\frac{\partial\overline{u_i}}{\partial x_j}+\frac{\partial\overline{u_j}}{\partial x_i})n_i dA+\iint_{S_2}\overline{u_j}\nu(\frac{\partial\overline{u_i}}{\partial x_j}+\frac{\partial\overline{u_j}}{\partial x_i})n_i dA\right]$$

Term 9 in Eq. (8b), representing physically the concept of the work done by the turbulence stresses, using the Boussinesq Hypothesis can be written as:

$$-\frac{1}{\rho g A_1 U_1}\left[-\iint_{S_1}\rho\overline{u_j}\overline{u_i'u_j'}\,n_i dA-\iint_{S_2}\rho\overline{u_j}\overline{u_i'u_j'}\,n_i dA\right]$$
$$\equiv-\frac{1}{gA_1U_1}\left[\iint_{S_1}2\nu_t\overline{s_{ij}u_j}\,n_i dA+\iint_{S_2}2\nu_t\overline{s_{ij}u_j}\,n_i dA\right] \quad (11)$$
$$\equiv-\frac{1}{gQ}\left[\iint_{S_1}\nu_t\left(\frac{\partial\overline{u_i}}{\partial x_j}+\frac{\partial\overline{u_j}}{\partial x_i}\right)\overline{u_j}\,n_i dA+\iint_{S_2}\nu_t\left(\frac{\partial\overline{u_i}}{\partial x_j}+\frac{\partial\overline{u_j}}{\partial x_i}\right)\overline{u_j}\,n_i dA\right]$$

It is necessary to mention that in the case of using *RSM*[4] model, term 9 is calculable without any changes in the initial form.

Term 6 in Eq. (8b), for which various concepts like the work done by the viscous shear stresses of the turbulent motion and the viscous diffusion of the turbulent energy have been considered by different researchers, is equalized as follows [16–19]:

$$-\frac{1}{\rho g A_1 U_1}\left[\iint_{S_1}\overline{\tau_{ij}'u_j'}n_i dA+\iint_{S_2}\overline{\tau_{ij}'u_j'}n_i dA\right]$$
$$=-\frac{1}{gQ}\left[\iint_{S_1}(\nu\frac{\partial k}{\partial x_i})n_i dA+\iint_{S_2}(\nu\frac{\partial k}{\partial x_i})n_i dA\right] \quad (12)$$

About term 8 in Eq. (8b) which consists of two terms of the pressure work due only to turbulence ($\overline{p'u_i'}$) and the transport of the turbulent kinetic energy by turbulent fluctuations (velocity triple correlation $\frac{\overline{u_i'u_j'u_j'}}{2}$), various researchers have generally considered the concept of the convective diffusion by turbulence of the total turbulence mechanical energy (turbulent diffusion), or the work done by the total dynamic pressure of turbulence and assumed that it is proportional to the turbulent kinetic energy (k) gradient [16–19], means:

$$-\frac{1}{\rho g A_1 U_1}\left[-\iint_{S_1}(\overline{p'u_i'}+\rho\frac{1}{2}\overline{u_i'u_j'u_j'})n_i dA-\iint_{S_2}(\overline{p'u_i'}+\rho\frac{1}{2}\overline{u_i'u_j'u_j'})n_i dA\right]\equiv$$
$$-\frac{1}{gQ}\left[\iint_{S_1}(\frac{\nu_t}{\sigma_k}\frac{\partial k}{\partial x_i})n_i dA+\iint_{S_2}(\frac{\nu_t}{\sigma_k}\frac{\partial k}{\partial x_i})n_i dA\right] \quad (13)$$

where $\sigma_k=1$. Following, the numerical simulations of the open-channel turbulent flows are performed to investigate the application of the developed relationships. In this regard, it should be noted that as mentioned earlier, the bases of the method presented in this study are theoretical analyses and numerical simulations. Based on these tools, the details of the total mechanical energy balance equation can be estimated without measurements.

[4] Reynolds stress model

2.2. Numerical Simulation

In this study, a Computational Fluid Dynamics (CFD) software, OpenFOAM, is used to solve the governing equations (momentum and mass conservation) by the finite volume discretization method with Reynolds stress turbulence model. An important issue is to know which solver is appropriate to use. In this paper, it is decided to use *pimpleFoam* and *gPimpleFoam* solvers (*gPimpleFoam* solver is developed by adding the gravitational acceleration g to *pimpleFoam*, that is transient solver for an incompressible single fluid) and treat the surface as a rigid lid (the same approach used by Pavanelli Lira [20], Liu and Xue [15], etc.).

2.2.1. Governing Equations

As mentioned earlier, in this study, Reynolds decomposition method are applied in governing equations. After substituting and time averaging, the following equations are obtained [19, 21]:

$$\frac{\partial(\rho\overline{u_i})}{\partial x_i} = 0 \tag{14}$$

$$\frac{\partial(\rho\overline{u_i})}{\partial t} + \frac{\partial(\rho\overline{u_i u_j})}{\partial x_j} = -\frac{\partial\overline{p}}{\partial x_i} + \frac{\partial}{\partial x_j}\left(\mu\frac{\partial\overline{u_i}}{\partial x_j} - \rho\overline{u_i' u_j'}\right) + \rho f_i \tag{15}$$

In Reynolds averaged Navier-Stokes (RANS) equations, in addition to the unknowns $\bar{u}_i$ and $\bar{p}$, there is also $-\rho\overline{u_i' u_j'}$ called Reynolds stress tensor. The *RSM* model is used to estimate the term, which its relation is as follows [14, 19]:

$$\frac{\partial(\rho\overline{u_i' u_j'})}{\partial t} + \frac{\partial(\rho\overline{u_k}\,\overline{u_i' u_j'})}{\partial x_k} = \underbrace{-\rho\overline{u_i' u_k'}\frac{\partial\overline{u_i}}{\partial x_k} - \rho\overline{u_j' u_k'}\frac{\partial\overline{u_j}}{\partial x_k}}_{G_{ij}} + \underbrace{\overline{p'\left(\frac{\partial u_i'}{\partial x_j} + \frac{\partial u_j'}{\partial x_i}\right)}}_{\Phi_{ij}} - \underbrace{\frac{\partial(\rho\overline{u_i' u_j' u_k'})}{\partial x_k}}_{D_{ij}} - \frac{2\rho\varepsilon\delta_{ij}}{3} \tag{16}$$

in which, G_{ij}, Φ_{ij} and D_{ij} are the Reynolds stress generation term, the pressure-strain correlations and the diffusion term, respectively. The turbulent kinetic energy k is calculated from $k = 0.5\overline{u_i' u_j'}$, and the turbulent kinetic energy dissipation rate ε is obtained from Eq. (17) [19, 22, 23]:

$$\frac{\partial(\rho\varepsilon)}{\partial t} + \frac{\partial(\rho\bar{u}_j\varepsilon)}{\partial x_j} = \frac{\partial}{\partial x_j}\left[\left(\mu + \frac{\mu_t}{\sigma_\varepsilon}\right)\frac{\partial\varepsilon}{\partial x_j}\right] + C_{\varepsilon 1}\frac{\varepsilon}{k}\left(2\mu_t\overline{s_{ij}}\frac{\partial\bar{u}_i}{\partial x_j}\right) - C_{\varepsilon 2}\rho\frac{\varepsilon^2}{k} \tag{17}$$

where the values of the coefficients are: $C_{\varepsilon 2} = 1.92$, $C_{\varepsilon 1} = 1.44$ and $\sigma_\varepsilon = 1.3$ [19].

2.2.2. Boundary Conditions

In this study, the boundary conditions are specified on all boundary faces of the domain. Fixed value for velocity at the inlet boundary and standard wall functions at the solid boundaries are used. The turbulent kinetic energy (k) and its dissipation rate (ε) at the inlet boundary are estimated by the following relations [24]:

$$k = 1.5(T_u U_0)^2 \tag{18}$$

$$\varepsilon = C_\mu^{\frac{3}{4}}\frac{k^{\frac{3}{2}}}{L} \tag{19}$$

where U_0 and T_u are the average inlet velocity and the turbulence intensity (typically 1–5% depending on upstream flow), respectively; C_μ is constant and = 0.09; and L = 0.07 of the

hydraulic depth [24]. Neumann boundary condition (zero gradient $\frac{\partial}{\partial n} = 0$) is applied at the outlet. Symmetry and dissipation boundary condition (turbulent damping similar to one in Celik and Rodi [25] for ε, considering a constant of a = 0.43) are adopted at the top of the channel.

2.2.3. Numerical Scheme

In this paper, Courant stability criterion is used to calculate the maximum time step. In other words, the time step is varied according to the maximum Courant number ($CFL = \Delta t \times \sum_{i=1}^{n=3} \frac{U_i}{\Delta X_i} \leq CFL_{max}$). *PIMPLE* algorithm for coupling the pressure-velocity is used.

In numerical simulations, first-order Euler discretization scheme for the time, linearUpwind for the advection terms, and Gauss linear interpolation method (central differencing) for the diffusion terms are used. The algebraic equations are solved by Gauss-Seidel iteration method in this paper. The simulations are carried out until steady conditions are achieved and then the calculated and experimental or numerical results are compared.

3. Results and Discussion

3.1. Verification

The tests considered for validation are the same as that described by Mamizadeh and Ayyoubzadeh [26, 27]. First, Mamizadeh and Ayyoubzadeh [26, 27] investigated three-dimensional turbulent flows in sudden expansions of rectangular channels based on Zhou [28]'s test (named test 1 in this study), using *FLUENT* software with coarse (9726 nodes and $\Delta x = \Delta y$ = 0.28), medium (68651 nodes and $\Delta x = \Delta y$ = 0.14) and fine mesh size (270291 nodes). The upstream channel is 1.4 *m* wide and 14 *m* long, and the downstream expanded channel is 2.8 *m* wide and 14 *m* long. There is no bed slope in the channel. The upstream inlet velocities, flow depth and Froude number are u = 0.63 *m/s*, v = 0, y = 0.2 *m* and Fr = 0.45, respectively. In addition, they constructed a laboratory flume with sudden expansion and the flow pattern was studied experimentally and numerically (test 2). The flume consists of two sections: section 1 has 5 *m* length, 0.16 *m* width, 0.30 *m* depth and no bed slope, and section 2 has a length of 10 *m*, a width of 0.96 *m* and a longitudinal slope of 2%. The upstream inlet discharge and the flow depth are Q = 0.0045 m^3/s and y = 0.3 *m*, respectively. In the simulations, the flow depth was considered constant and the variations of the free surface were not considered [26, 27].

In the present study, according to what was mentioned, once the validation is performed by considering the constant depth, which is in compliance with the assumption of Henderson [9] for the energy loss calculation in sudden expansions, and once again it is carried out with calculating the downstream depth from the relationship provided by Najafi-Nejad-Nasser and Li [6], that led to achieve 0.21 *m* for the downstream depth with 5% increase in depth in comparison to the upstream depth of the transition. Under given condition, it can be assumed that the effect of the expansion on the free surface is not significant and major flow changes occur across the channel. In the simulation process, grid characteristics is very important because the mesh influences the accuracy, convergence, and speed of the simulation. In this study, the selected mesh is non-uniform and fine enough especially near the critical zone like sudden expansion and near the walls. Considering the computational domain similar to Fig. 2 for test 1, the number of cells in the longitudinal, lateral and vertical directions for the open-channel expansion with the expansion ratio of b_2/b_1 = 2, are selected 305 × 40 × 22 in upstream channel and 117 × 90 × 22 in downstream channel. The total cells numbers are 500060 (Fig. 2).

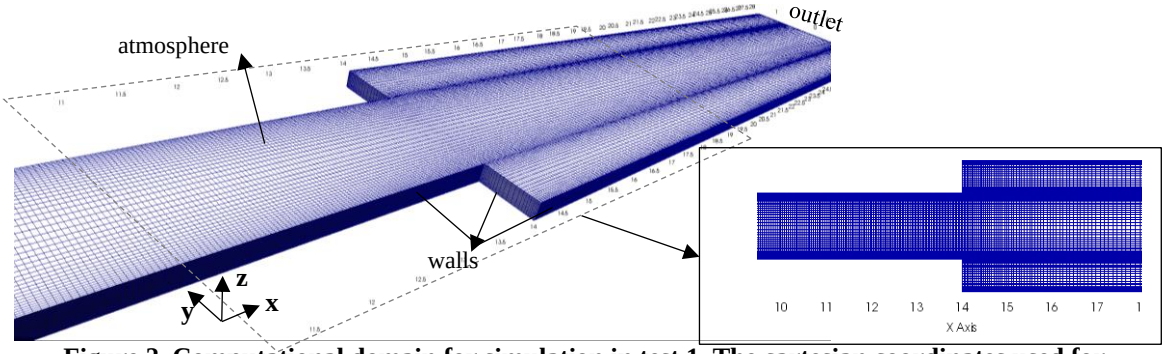

Figure 2. Computational domain for simulation in test 1. The cartesian coordinates used for computational domain and grid characteristics with ensuring fine mesh near the critical zone like sudden expansion and near the walls

Fig. 3 compares the results of the numerical simulation in this study with the data of Mamizadeh and Ayyoubzadeh [26, 27] in test 1. The velocity profiles across the channel are presented before and after the transition in Fig. 3*a* and Fig. 3*b*, respectively. According to these figures, it can be noted that the results in two states of constant and inconstant depths are consistent together and also similar to Mamizadeh and Ayyoubzadeh [26, 27]'s results (mean error percentages of 0.11% and 2.68% with the velocity profiles by fine mesh before and after transition [26, 27], respectively). The reason for the small differences can be found in the difference of the number of cells in the simulation process in this study (500060 cells) with Mamizadeh and Ayyoubzadeh [26, 27]'s study, and also the difference between the turbulence models used in the present study (*RSM*) and the study of Mamizadeh and Ayyoubzadeh [26, 27] (*k*-*ε*).

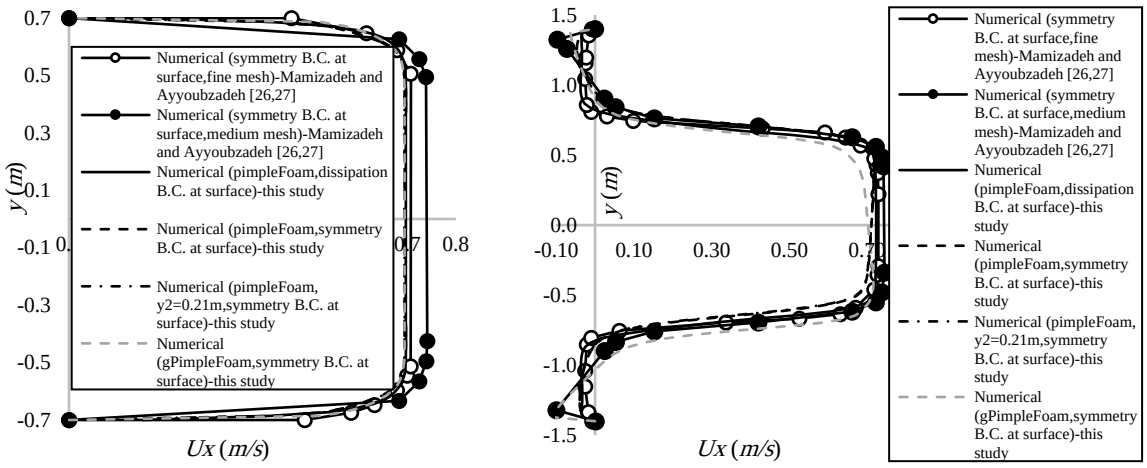

(*a*) *x* = 10 (*m*) **(*b*) *x* = 15 (*m*)**

Figure 3. Comparison of the simulated results in this study with the numerical data of Mamizadeh and Ayyoubzadeh [26, 27] in test 1

It should be noted that at higher iterations, the velocity distribution shows that after expansion, the flow diverts to one side and an asymmetric flow pattern occurs (Fig. 3*b*), that is

also shown clearly in Fig. 4 (in which the simulated velocity vectors at the free surface in this study are compared with those of Zhou [28]'s test). The reason for the occurrence of the asymmetric flow pattern in symmetric sudden-expansion channel is related to the greater expansion ratio than 1.5 (b_2/b_1 = 2.0). This result is in agreement with both experimental observations and theoretical analyses by the previous researchers [28, 29]. However, it was not found in the numerical simulation of Mamizadeh and Ayyoubzadeh [26, 27] with fine mesh.

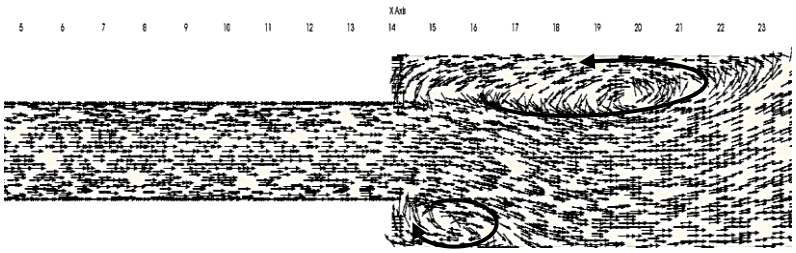

(*a*) Simulated velocity vectors at the free surface in this study (*gPimpleFoam - symmetry B.C at surface*)

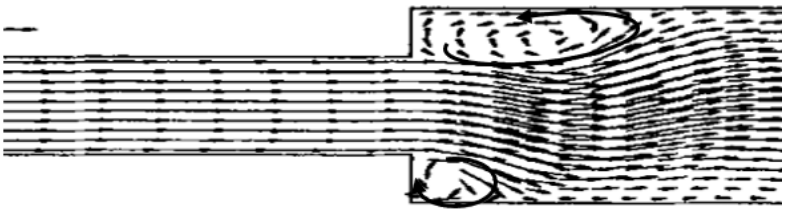

(*b*) velocity vectors in symmetric sudden-expansion channel in Zhou [28]'s test

Figure 4. Comparison of the simulated velocity vectors in this study with those of Zhou [28]'s test

Relatively acceptable compliance of the results presented in this section makes it possible to further use the simulation results to estimate the mechanical energy loss and other quantities. It is noteworthy that in the studies of Mamizadeh and Ayyoubzadeh [26, 27] and Zhou [28], there is no value for the energy loss. Hence, Eq. (20) proposed by Henderson [9] for the open-channel with sudden expansion is used as an initial value for the validation and the results are presented in Table 1.

$$h_L = \frac{U_1^2}{2g}\left[\left(1-\frac{b_1}{b_2}\right)^2 + \frac{2Fr_1^2 b_1^3(b_2-b_1)}{b_2^4}\right] \tag{20}$$

Table 1. The difference percentage between the calculated energy losses from the direct relationship in this study and the losses from Henderson [9]'s relationship (Eq. 20) for test 1

h_w from Eq. (8*a*)	h_w from Eq. (8*a*) with Δh_{sfd} from Eq. (8*b*) (without term 10)	h_w from Eq. (8*a*) with Δh_{sfd} from Eq. (8*b*) (without term 10) and $\Delta\beta k/g$
	pimpleFoam- Symmetry B.C. at surface	
0.42 %	2.42 %	4.75 %
	gPimpleFoam - Symmetry B.C. at surface	
8.83 %	11.27 %	13.29 %

The results indicate that in this case study (test 1), despite the differences in the parameters

involved in the compared energy loss relationships, the computational losses from the direct relationships in the present study have a relatively appropriate agreement with the losses from Henderson [9]'s relationship in symmetric sudden-expansion channels. The reason for the differences can be found in the presence of the turbulence parameters taken into account in the total mechanical energy equation developed in this study which were not considered in Eq. (20). The details will be discussed later.

In the next step, in order to further investigate the application of the direct relationships for the energy loss estimation with more details of turbulence parameters extracted from the complete form of the mechanical energy equation developed in this study, the relationships are applied using the simulation results based on the experimental data in laboratory flume of Mamizadeh and Ayyoubzadeh [26, 27] (test 2), in which the flow characteristics were presented earlier. The steps of the examination of the results are the same as the previous section (it should be noted that in this section, the developed solver named *gPimpleFoam* in this study is only used). It means that the velocity distribution is first investigated (Fig. 5). It is noteworthy that the symmetric flow pattern was obtained in the numerical simulation of Mamizadeh and Ayyoubzadeh [26, 27] (Fig. 5a), which did not match to the asymmetric flow pattern in the experimental observations [26, 27]. In the present study, the flow pattern formed up to $T = 250s$ consists of two symmetrical vortexes on both sides of the expansion and a maximum flow velocity in the central line that is similar to Mamizadeh and Ayyoubzadeh [26, 27] (Fig. 5*a*). However, the flow diverts to one side and an asymmetric flow pattern occurs after $T = 250s$, which has also been observed in the experiments of Mamizadeh and Ayyoubzadeh [26, 27]. As mentioned earlier, the experimental and theoretical studies of other researchers also confirm this [28, 29].

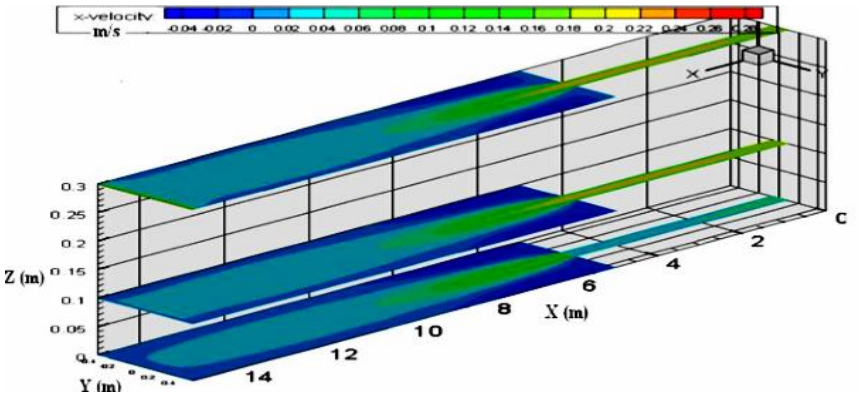

(*a*) *x*-velocity distribution at different depths from simulation by Mamizadeh and Ayyoubzadeh [26, 27]

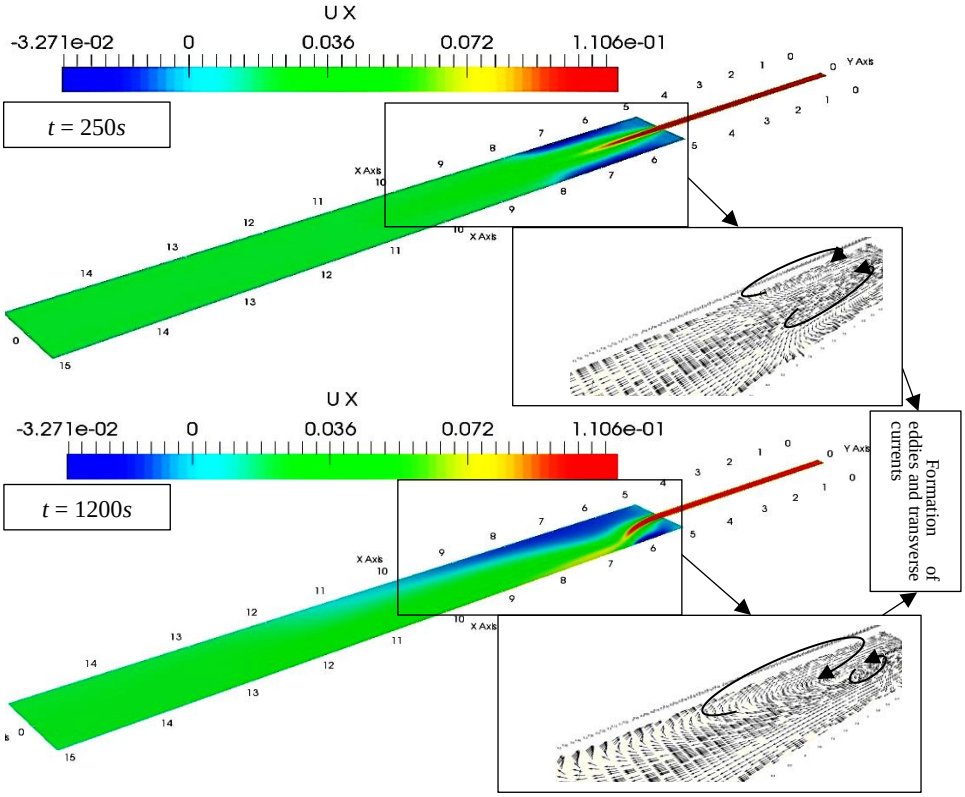

(*b*) *x*-velocity distribution at surface obtained from the numerical simulation in this study

Figure 5. Comparison of the simulated results in this study with those of Mamizadeh and Ayyoubzadeh [26, 27] in test 2

In the following, the energy loss coefficients calculated from Eq. (21), in which the losses are obtained from the direct relationship of $h_w+\Delta h_{sfd}+\Delta\beta k/g$ using Eq. (8) in this study (which is equivalent to the difference of terms 1 and 2 in Eq. 7 between two cross-sections) and the previous relationships such as Eqs. (20, 22-25) [2, 4, 9, 10], are compared and the results are presented in Fig. 6.

$$k_e = \frac{h_L}{(\frac{U_1{}^2}{2g})} \quad (21)$$

$$h_L = \frac{U_1^2}{2g}\left(1 - \frac{b_1}{b_2}\right)^2 = \frac{(U_1 - U_2)^2}{2g} \quad (22)$$

$$h_L = K\left(\frac{U_1^2}{2g} - \frac{U_2^2}{2g}\right), K = 0.75 \quad (23)$$

$$h_L = (y_1 + \alpha_1 \frac{U_1^2}{2g}) - (y_2 + \alpha_2 \frac{U_2^2}{2g}) \quad (24)$$

$$h_L = \frac{U_1^2}{2g}(1 - \frac{b_1 y_1}{b_2 y_2})^{1.2} \quad (25)$$

As shown in Fig. 6, the lower estimation of the energy loss coefficient from Eq. (20) in comparison to the loss coefficients from the other equations is clearly seen, that has been also shown by previous researchers [10, 12]. A possible explanation is that the restriction that Fr_1 is small enough for Fr_1^4 and higher powers to be neglected, needed to derive Eq. (20) (and Eq. 22), is not valid in this study.

Nevertheless, the results of the validations in this section indicate that there is relatively appropriate agreement between the energy loss obtained from the direct method of calculating the available terms of the mechanical energy loss using the simulation results in this study and the values from the theoretical and experimental relationships in channels with sudden expansions. Therefore, other methods for the energy loss estimation with more details of the turbulence parameters in this study can be used further with more confidence (Table 2).

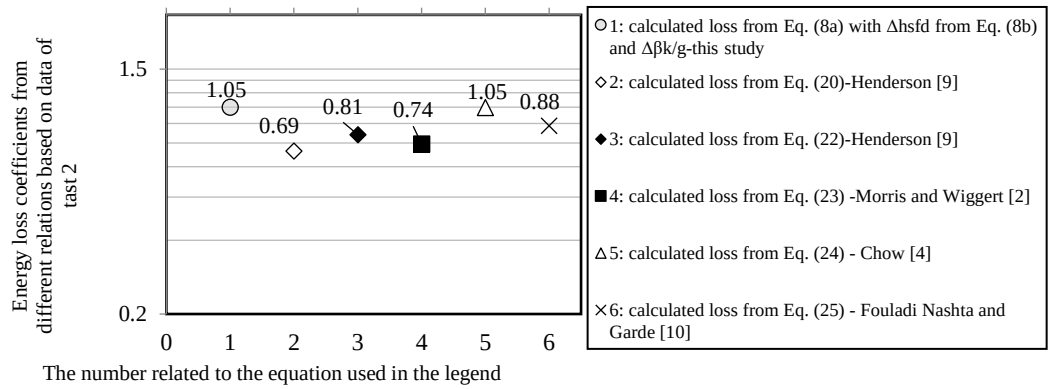

Figure 6. Comparison of the energy loss coefficients from the different loss relationships based on Mamizadeh and Ayyoubzadeh [26, 27]'s experimental data with the coefficient obtained from the direct relationship of the energy loss in this study using the simulation results from *gPimpleFoam* by dissipation B.C. at surface

For this purpose, in the following, the difference percentage between the energy loss calculated from the direct relationships in this study and the energy loss from the common theoretical and semi-empirical relationships is obtained and presented in Table 2. It should be noticed that the reason for the discrepancy between the losses from the mechanical energy equation improved in this study and the previous mechanical energy equations is clearly related

to the consideration of more details of the turbulence parameters in the proposed form of the total mechanical energy equation, including the turbulent kinetic energy variation, the work done by turbulence stresses and the turbulent diffusion, etc. that have not been considered in the previous equations.

As mentioned earlier, for a closer comparison, the losses obtained from considering Δh_{sfd} (Eq. 8*b*) with the direct loss relationship (Eq. 8*a*) should be compared to the losses from Eq. (24), under which a relatively acceptable percentage difference is obtained (see Table 2. column 3, the last two rows in each section). One reason for the difference in computational losses from $h_w+\Delta h_{sfd}+\Delta\beta k/g$ in the present study with Eq. (22) extracted from Eq. (20) with similar assumptions is previously discussed. Another reason can be found in the assumption of uniform velocity ($\alpha_1 = \alpha_2 = 1$) in Eq. (22) [9], that is not used in the present study. In addition, despite the differences in the parameters involved in the compared energy loss relationships, the relatively appropriate agreement between the calculated losses in this study and the losses from the semi-empirical relationship by Fouladi Nashta and Garde [10] in the open-channel expansion is clearly seen in most cases.

Table 2. The difference percentage of the calculated energy losses from the direct relationships in this study with the energy losses from the common theoretical and semi-empirical relationships based on Mamizadeh and Ayyoubzadeh [26, 27]'s data (test 2)

	(1)The difference percentage with the loss from Eq. (22) [9]	(2)The difference percentage with the loss from Eq. (25) [10]	(3)The difference percentage with the loss from Eq. (24) [4]
	gPimpleFoam - Symmetry B.C. at surface		
h_w from Eq. (8*a*)	6.13%	2.39%	17.75%
h_w from Eq. (8*a*) with Δh_{sfd} (without term 10)	4.83%	3.59%	18.76%
h_w from Eq. (8*a*) with Δh_{sfd} (without term 10) and $\Delta\beta k/g$	3.61%	4.71%	19.70%
h_w from Eq. (8*a*) with Δh_{sfd}	31.98%	21.39%	2.29%
h_w from Eq. (8*a*) with Δh_{sfd} and $\Delta\beta k/g$	30.76%	20.27%	1.34%
Average	**15.46%**	**10.47%**	**11.97%**

	(1)The difference percentage with the loss from Eq. (22) [9]	(2)The difference percentage with the loss from Eq. (25) [10]	(3)The difference percentage with the loss from Eq. (24) [4]
	gPimpleFoam - Dissipation B.C. at surface		
h_w from Eq. (8*a*)	5.91%	2.59%	17.91%
h_w from Eq. (8*a*) with Δh_{sfd} (without term 10)	4.63%	3.77%	18.91%
h_w from Eq. (8*a*) with Δh_{sfd} (without term 10) and $\Delta\beta k/g$	3.43%	4.88%	19.84%
h_w from Eq. (8*a*) with Δh_{sfd}	30.52%	20.04%	1.16%
h_w from Eq. (8*a*) with Δh_{sfd} and $\Delta\beta k/g$	29.32%	18.93%	0.23%
Average	**14.76%**	**10.04%**	**11.61%**

3.2. Contribution of the different parameters to the total mechanical energy loss of 3-D turbulent flows in open-channel expansions

An important result that can be deduced from the calculations based on Eq. (8*a*) is that the contribution of the turbulent energy dissipation (term 7) is dominant and the contribution of the viscous dissipation of the mean flow (term 5) to the mechanical energy loss of turbulent flows is negligible (Table 3).

Table 3. The contribution of the viscous dissipation and turbulent energy dissipation to the turbulent flow energy loss based on the direct relationship (Eq. 8*a*) in this study

	contribution of turbulent energy dissipation (term 7)	contribution of viscous dissipation (term 5)
calculated loss using *pimpleFoam* solver and dissipation B.C. at surface (based on the data of test 1)	96.77 %	3.23 %
calculated loss using *gPimpleFoam* solver and dissipation B.C. at surface (based on the data of test 2)	95.89%	4.11%
calculated loss using *gPimpleFoam* solver and symmetry B.C. at surface (based on the data of test 2)	95.90%	4.10%

This result can also be found in the case of using the direct Eq. (8*a*) by considering other turbulence parameters. For example, in Fig. 7, the effect of the different parameters of the turbulent flow on the mechanical energy loss shows the dominant effect of the dissipation rate of turbulence kinetic energy (term 7) that is converted into heat. The effects of the turbulent diffusion (term 8), the work done by viscus shear stresses of the turbulent motion (viscous diffusion named term 6 in this study) and the work done by viscus stresses (term 4) on the energy loss of turbulent flow in open-channel transitions is negligible. In other hand, the values of $\Delta\beta k/g$ and Δh_{sfd} which have been omitted in the previous studies indicate the mechanical energy transformation which is equal to zero in uniform turbulent flows (Liu et al. [14]). Therefore, it can be found that these terms are related to the changes of the flow cross-sectional area (channel geometry) and show the effect of non-homogeneity and anisotropy of turbulence that generate the turbulence-driven secondary currents.

In general, there are some shortcomings in the Bernoulli's equation which is still being used: (1) The variations of the different turbulence parameters such as the turbulent kinetic energy, the work done by turbulence stresses, etc. cannot be evaluated; (2) The assumption of hydrostatic pressure distribution cannot be reasonable for the 3-D turbulent flows because of the existence of the secondary currents; (3) A relationship of the mechanical energy loss based on the turbulence parameters cannot be determined directly.

Investigation of the results in the present study show that, the application of the new energy equation and the direct energy loss relationship for incompressible turbulent flows derived in this paper can avoid the shortcomings mentioned above.

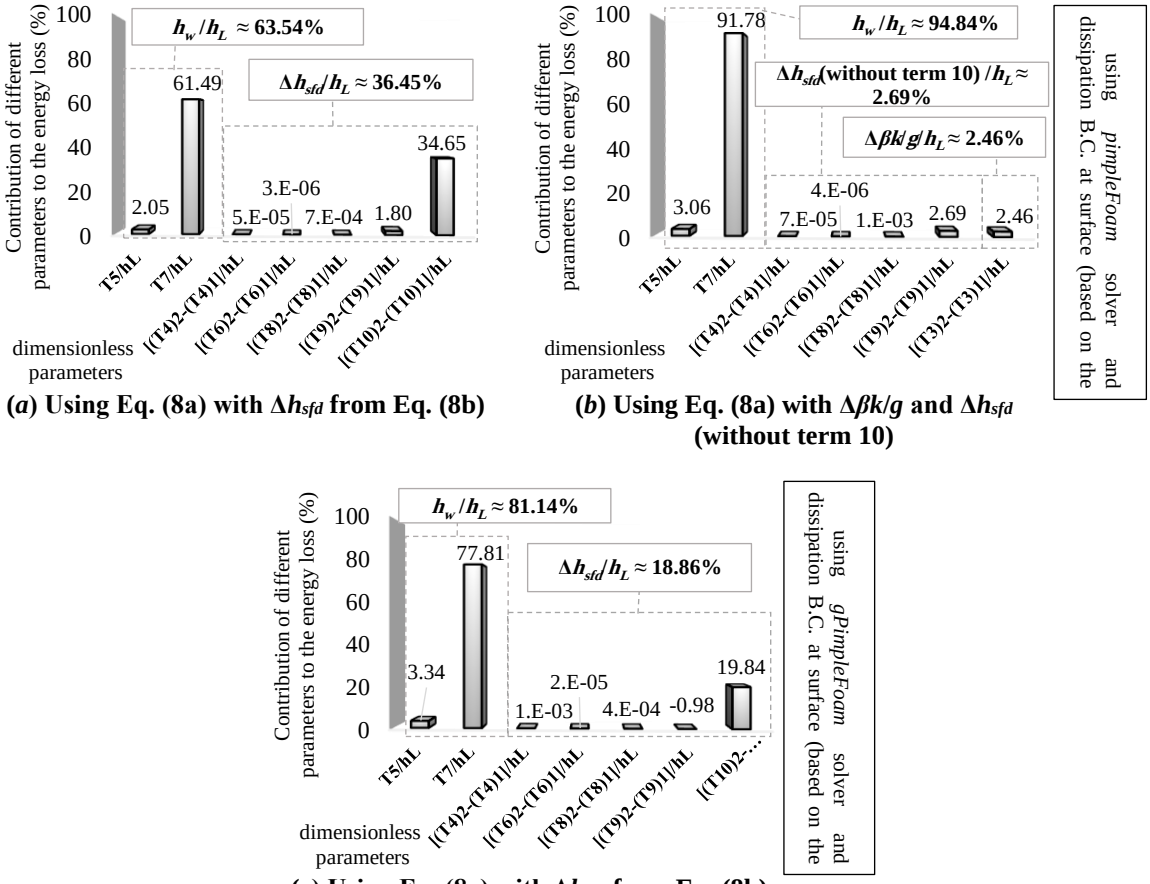

(*a*) Using Eq. (8a) with Δh_{sfd} from Eq. (8b) **(*b*) Using Eq. (8a) with $\Delta\beta k/g$ and Δh_{sfd} (without term 10)**

(*c*) Using Eq. (8a) with Δh_{sfd} from Eq. (8b)

Figure 7. Contribution of the different parameters to the turbulent flow energy loss (h_L) along the downstream expanded channel using the direct energy loss relationships and the simulation results in this study

3.3. Formulation of the Manning roughness coefficient based on the turbulence parameters

Dividing Eq. (8*a*) by the distance between the upstream and downstream cross-sections of the transition (l), we will have:

$$S_f = \frac{1}{\rho g Q l}\iiint_V (\overline{\tau_{ij} s_{ij}} + \overline{\tau'_{ij} s'_{ij}})dV \quad (26)$$

Where, S_f denotes the energy slope related to the flow mechanical energy loss. By applying Eq. (26) and Manning flow resistance relation as $S_f = \frac{n^2 U^2}{R^{\frac{4}{3}}}$, Eq. (27) is achieved for Manning roughness coefficient which is usually determined empirically or experimentally, based on the turbulence parameters:

$$n = \frac{R^{\frac{2}{3}}}{(U_1^2 \rho g Q l)^{\frac{1}{2}}}\left[\iiint_V (\overline{\tau_{ij} s_{ij}} + \overline{\tau'_{ij} s'_{ij}})dV\right]^{\frac{1}{2}} = \frac{R^{\frac{2}{3}}}{(U_1^2 \rho g Q l)^{\frac{1}{2}}}\left[\iiint_V (2\mu\overline{s_{ij} s_{ij}} + \rho\varepsilon)dV\right]^{\frac{1}{2}} \quad (27)$$

Using Eq. (27) in which the Manning roughness coefficient is calculated based on the energy

loss relationship in test 1, the value of n = 0.0198 by considering symmetry B.C. for all parameters at the free surface and the value of n = 0.0226 by considering the dissipation B.C. at the free surface are obtained, that are in agreement with the roughness coefficient proposed in Zhou [28]'s test (n = 0.02), and indicate the appropriate performance of the above relationship.

4. Conclusions

The governing equations of the flow, including the energy balance equation have been previously defined in Hydraulics and Fluid Mechanics. In the previous studies, simplifying assumptions have been used, which limit the application of the energy equation. In this study, a complete form of the total mechanical energy balance equation is investigated, in which by eliminating the previous assumptions, it is possible to analyze more details of turbulent flows with the presence of the secondary currents having three-dimensional behavior.

Explicit relationships for the mechanical energy loss of the turbulent flow and the roughness coefficient in the resistance relationship that have usually been determined empirically or experimentally are extracted from the energy equation, the application of which led to avoid the shortcomings of the previous relationships.

After developing the analytical relationships, three-dimensional numerical simulations are performed for turbulent flows in open-channel expansions. Initial validation of the results shows that asymmetric flow pattern occurs for b_2/b_1 values greater than 1.5, when the flow expands in channel expansions. Then, the analytical model is used to calculate the energy losses and compare them with the energy losses of the common analytical and semi-empirical relationships. The differences are related to consider the details of the turbulence parameters in the present energy equation, which were not taken into account in the previous mechanical energy equations. The acceptable results indicate that in the field of modeling turbulent flow in open-channel transitions and calculating the energy losses with more details of turbulence parameters, the proposed model has capability and relatively high accuracy.

Regarding to the effect of the different turbulence parameters on the energy loss, the obtained results indicate that the work done by viscous shear stresses, the viscous diffusion of the turbulent energy and the turbulent diffusion can be neglected, while the dissipation rate of turbulence kinetic energy, the variations of the turbulent kinetic energy and the work done by the turbulence stresses have relatively significant effects on the energy loss. In other words, in order to more accurate study the process of the energy loss in turbulent flows in open-channel transitions, it is better to use the total mechanical energy equation derived in this study, which includes the details of 3-D turbulent flows.

References

1. Hager, W. H., (2010). Wastewater hydraulics: Theory and practice: Second edition.
2. Morris, H. M. and Wiggert, J. M., (1972). Applied hydraulics in engineering, Wiley.
3. French, R. H., (1986). open-channel hydraulics, MacGraw-Hill.
4. Chow, V. T., (1959). Open Channel Hydraulics, Mcgraw-Hill Company.
5. Mahmoudi, M., Tabatabai, M. R. M., and Nadoushani, S. M., (2019). An analytical approach to the estimation of optimum river channel dimensions, Scientia Iranica, 26(3A), pp: 1169–1181.
6. Nezu, I. and Nakagawa, H., (1989). Turbulent structure of backward-facingstep flow and coherent vortex shedding from reattachment in open chan-nel flows, inTurbulent Shear

Flows: Selected Papers From the SixthInternational Symposium on Turbulent Shear Flows, pp: 313–337, Springer, Berlin.
7. Amara, L., Berreksi, A. and Achour, B., (2017). Quasi-2D model for computation of supercritical free surface flow in sudden expansion, Appl. Math. Model., 46, pp: 396–407.
8. Haque, A., (2008). Some Characteristics of Open Channel Transition Flow, M.Sc. Thesis, Civil Engineering, Concordia University.
9. Henderson, F. M., (1966). Macmillan Publishing Co, Inc. New York.
10. Fouladi Nashta, C. and Garde, R. J., (1988). Subcritical flow in rigid-bed open channel expansions, J. Hydraul. Res., 26(1): pp. 49–65.
11. Basak, B. C.and Alauddin, M., (2010). Efficiency of an expansive transition in an open channel subcritical flow, DUET Journal, Dhaka Univ. Eng. Technol., 1(1): pp. 27–32.
12. Najafi-Nejad-Nasser, A., and Li, S. S., (2015). Reduction of flow separation and energy head losses in expansions using a hump. Journal of Irrigation and Drainage Engineering, 141(3): pp. 04014057-1 – 04014057-9.
13. Artichowicz, W. and Sawicki, J. M., (2017). Determination of mechanical energy loss in steady flow by means of dissipation power, Arch. Hydro-Engineering Environ. Mech., 64(2): pp. 73–85.
14. Liu, S., Fan, M., and Xue, J., (2014). The mechanical energy equation for total flow in open-channels. Journal of Hydrodynamics, 26(3): pp. 416–423.
15. Liu, S., and Xue, J., (2016). Theoretical analysis and numerical simulation of mechanical energy loss and wall resistance of steady open-channel flow. Journal of Hydrodynamics, 28(3): pp. 489–496.
16. Hinze, J. O., (1975). Turbulence McGraw. McGraw-Hill Publishing Co., New York.
17. Nezu, I. and Nakagawa, H., (1993). Turbulence in open-channel flows, Balkema, Rotterdam: IAHR Monograph.
18. Førde, O. Ø., (2012). Analysis of the turbulent energy dissipation, M.Sc. Thesis, Norwegian University of Science and Technology.
19. Wilcox, D. C., (1998). Turbulence modeling for CFD (Vol. 2). DCW industries La Canada, CA.
20. Pavanelli Lira, V., (2014). Numerical modeling of a 90° open- channel confluence flow using openfoam cfd, M.Sc. Thesis, Federal University of Minas Gerais.
21. Salih, S. Q., Aldlemy, M. S., Rasani, M. R., Ariffin, A. K., Ya, T. M. Y. S. T., Al-Ansari, N., Yaseen, Z. M., and Chau, K. W., (2019). Thin and sharp edges bodies-fluid interaction simulation using cut-cell immersed boundary method. Engineering Applications of Computational Fluid Mechanics, 13(1): pp. 860–877.
22. Asnaashari, A., Akhtari, A. A., Dehghani, A. A. and Bonakdari, H., (2018). Effect of Inflow Froude Number on Flow Pattern in Channel-Expansive Transitions, J. Irrig. Drain. Eng., 142, (1); pp. 06015004-1 – 06015004-5.
23. Abdo, K., Riahi-Nezhad, C. K., and Imran, J., (2018). Steady supercritical flow in a straight-wall open-channel contraction. Journal of Hydraulic Research, 57(5): pp. 647–661.

24. Versteeg, H. K., and Malalasekera. W., (2016). An Introduction to Computational. Fluid Dynamics. The finite volume method. London, Second Edition.
25. Celik, I., and Rodi, W., (1984). Simulation of free-surface effects in turbulent channel flows. Physicochemical Hydrodynamics, 5(3–4): pp. 217–227.
26. Mamizadeh, J., and Ayyoubzadeh, S. A., (2012b). Simulation of flow pattern in open channels with sudden expansions. Research Journal of Applied Sciences, Engineering and Technology, 4(19): pp. 3852–3857.
27. Mamizadeh, J., and Ayyoubzadeh, S., (2012a). Numerical and Experimental Simulation of Flow Pattern in Sudden and Gradual Canal Expansions, Journal of Engineering and Applied Sciences, 7(6): pp. 389-394.
28. Zhou, J. G., (1995). Velocity-depth coupling in shallow-water flows, Journal of Hydraulic Engineering, 121(10), 717–724.
29. Graber, S. D., (1982). Asymmetric flow in symmetric expansions, J. Hydraul. Div., vol. 108(10): pp. 1082–1101.